

1 Substantial ozone enhancement over the North China Plain from
2 increased biogenic emissions due to heat waves and land cover in
3 summer 2017

4 Mingchen Ma¹, Yang Gao^{1,2*}, Yuhang Wang^{3*}, Shaoqing Zhang^{2,4,5,6}, L. Ruby Leung⁷, Cheng
5 Liu^{8,9,10,11*}, Shuxiao Wang¹², Bin Zhao¹³, Xing Chang¹², Hang Su¹⁴, Tianqi Zhang¹, Lifang Sheng⁶,
6 Xiaohong Yao^{1,15}, Huiwang Gao^{1,15}

7
8 ¹Key Laboratory of Marine Environment and Ecology, Ministry of Education/Institute for Advanced Ocean
9 Study, Ocean University of China, Qingdao 266100, China

10 ²Qingdao National Laboratory for Marine Science and Technology, Qingdao, 266237, China

11 ³School of Earth and Atmospheric Sciences, Georgia Institute of Technology, Atlanta, GA 30332

12 ⁴Key Laboratory of Physical Oceanography, Ministry of Education/Institute for Advanced Ocean Study,
13 Ocean University of China, Qingdao 266100, China

14 ⁵International Laboratory for High-Resolution Earth System Prediction (iHESP), Qingdao, 266237, China

15 ⁶College of Oceanic and Atmospheric Sciences, Ocean University of China, Qingdao 266100, China

16 ⁷Atmospheric Sciences and Global Change Division, Pacific Northwest National Laboratory, Richland,
17 Washington, 99354, USA

18 ⁸Key Lab of Environmental Optics and Technology, Anhui Institute of Optics and Fine Mechanics, Hefei
19 Institutes of Physical Science, Chinese Academy of Sciences, Hefei, 230031, China

20 ⁹School of Earth and Space Sciences, University of Science and Technology of China, Hefei, 230026,
21 China

22 ¹⁰Center for Excellence in Regional Atmospheric Environment, Institute of Urban Environment, Chinese
23 Academy of Sciences, Xiamen, 361021, China

24 ¹¹Anhui Province Key Laboratory of Polar Environment and Global Change, USTC, Hefei, 230026, China

25 ¹²State Key Joint Laboratory of Environment Simulation and Pollution Control, School of Environment,
26 Tsinghua University, Beijing 100084, China

27 ¹³Joint Institute for Regional Earth System Science and Engineering and Department of Atmospheric and
28 Oceanic Sciences, University of California, Los Angeles, CA 90095, USA

29 ¹⁴Max Planck Institute for Chemistry, Multiphase Chemistry Department, D-55128 Mainz, Germany

30 ¹⁵Laboratory for Marine Ecology and Environmental Science, Qingdao National Laboratory for Marine
31 Science and Technology, Qingdao 266237, China

32 *To whom correspondence to: yanggao@ouc.edu.cn, yuhang.wang@eas.gatech.edu, chliu81@ustc.edu.cn

33

34
35
36
37
38
39
40
41
42
43
44
45
46
47
48
49
50
51
52
53
54
55
56
57
58

Abstract

In the summer of 2017, heavy ozone pollution swamped most of the North China Plain (NCP), with the maximum regional average of daily maximum 8-h ozone concentration (MDA8) reaching almost 120 ppbv. In light of the continuing reduction of anthropogenic emissions in China, the underlying mechanisms for the occurrences of these regional extreme ozone episodes are elucidated from two perspectives: meteorology and biogenic emissions. The significant positive correlation between MDA8 ozone and temperature, which is amplified during heat waves concomitant with stagnant air and no precipitation, supports the crucial role of meteorology in driving high ozone concentrations. We also find that biogenic emissions are enhanced due to factors previously not considered. During the heavy ozone pollution episodes in June 2017, biogenic emissions driven by high vapor pressure deficit (VPD), land cover change and urban landscape yield an extra mean MDA8 ozone of 3.08, 2.79 and 4.74 ppbv, respectively over the NCP, which together contribute as much to MDA8 ozone as biogenic emissions simulated using the land cover of 2003 and ignoring VPD and urban landscape. In Beijing, the biogenic emission increase due to urban landscape has a comparable effect on MDA8 ozone to the combined effect of high VPD and land cover change between 2003 and 2016. In light of the large effect of urban landscape on biogenic emission and the subsequent ozone formation, the types of trees may be cautiously selected to take into account of the BVOC emission during the afforestation of cities. This study highlights the vital contributions of heat waves, land cover change and urbanization to the occurrence of extreme ozone episode, with significant implications for ozone pollution control in a future when heat wave frequency and intensity are projected to increase under global warming.

Keywords

Ozone pollution, heat waves, biogenic emission, land cover change, urban landscape

59 **1 Introduction**

60 In recent decades, China has been facing severe air pollution issues, particularly for the winter
61 PM_{2.5} and summer ozone (Zheng et al., 2015; Cheng et al., 2016; Zhao et al., 2016). It has been
62 noted that the mean concentration of PM_{2.5} has generally decreased in the past few years but the
63 concentration of ozone shows an increasing trend (Li et al., 2017b; Wang et al., 2017; Chen et
64 al., 2018a; Li et al., 2019), suggesting a greater urgency for ozone pollution control. For
65 instance, Li et al. (2017b) revealed an increase of annual mean ozone in 2016 by 11 μg/m³
66 compared to 2014 in China. Lu et al. (2018) found a 3.7-6.2% increase per year in the mean
67 ozone concentration over 74 cities in China from 2013 to 2017. Since ozone is harmful to both
68 human health (Soriano et al., 2017) and vegetation (Emberson et al., 2009; Avnery et al., 2011),
69 it is vital to investigate the possible mechanisms related to high ozone concentrations. Based on
70 ozone observations from 2013-2017, the North China Plain (NCP, an area about 400,000 km² in
71 size with Beijing located on its northeast edge, 35°-42° N 112°-119° E), is identified as the area
72 with the most severe ozone pollution in China compared to other regions such as the Yangtze
73 River Delta and Pearl River Delta, possibly linked to the stimulation effect from enhanced
74 hydroperoxy radicals (HO₂) due to reduction in aerosol sink resulting from the decrease of PM_{2.5}
75 during this period (Li et al., 2019). Chen et al. (2019) investigated the impact of meteorological
76 factors such as temperature, wind speed and solar radiation on ozone pollution from 2006-2016
77 and noted that the severe ozone events in June 2017 around Beijing stand out and suggested a
78 possible connection with the abnormal meteorological conditions. These studies motivated a
79 need for a better understanding of the high ozone problem over NCP.

80 Tropospheric ozone is closely related to both anthropogenic emissions and biogenic
81 emissions, including volatile organic compounds (VOCs) and nitrogen oxides (NO_x) (Sillman,
82 1995, 1999; Tonnesen and Dennis, 2000; Xing et al., 2011; Fu et al., 2012). In the past few years
83 (i.e., 2012-2017), anthropogenic emissions such as NO_x continued to decrease (Liu et al., 2016)
84 and anthropogenic VOCs changed little (Zhao et al., 2018; Zheng et al., 2018; Li et al., 2019).
85 Biogenic VOCs (BVOC) were reported to enhance hourly ozone by 3-5 ppbv in NCP, especially
86 in areas north of Beijing, based on a two-day simulation from July 31 to August 1, 1999 (Wang
87 et al., 2008). The annual BVOC emission in this area increased by 1-1.5% per year from 1979-
88 2012 (Stavrakou et al., 2014) due to changes of land use and climate. Broadleaf trees in general

89 have a higher emission rate of BVOC than grass, shrub and crops (Guenther et al., 2012). A
90 dramatic increase of forest (trees) coverage is evident in the last 20 years over NCP (Chen et al.,
91 2018b), partly attributable to the “Three-north Forest Protection Project”. For example, trees
92 planted before the 2008 Olympic Games doubled the BVOC emissions in Beijing from 2005 to
93 2010 (Ghirardo et al., 2016). Urban landscape may even emit more BVOC than natural forest
94 because of favorable conditions such as lower tree densities and better light illumination (Ren et
95 al., 2017). Ren et al. (2017) found that BVOC emitted by urban landscape accounted for 15% of
96 total BVOC emissions in Beijing in 2015. Over highly polluted urban areas of the NCP, ozone
97 production is highly sensitive to VOCs emissions (Liu et al., 2012; Han et al., 2018). Therefore,
98 elevated BVOC emissions can greatly enhance ozone formation in NCP.

99 Besides emissions, tropospheric ozone is also closely related to meteorological conditions,
100 such as heat waves (Gao et al., 2013; Fiore et al., 2015; Otero et al., 2016), low wind speed and
101 stagnant weather (Jacob and Winner, 2009; Sun et al., 2017; Zhang et al., 2018). Weather
102 conditions concomitant with heat waves including high temperature, low wind speed, and little
103 cloud coverage may enhance ozone production (Jaffe and Zhang, 2017; Pu et al., 2017; Sun et
104 al., 2019). At the same time, such meteorological conditions also promote emissions of BVOC
105 and ozone formation (Zhang and Wang, 2016). Using a global model, Fu and Liao (2014)
106 suggested a slight-to-moderate increase of biogenic isoprene west and north of Beijing due to
107 land cover and land use alone, and an even more obvious increase when meteorological changes
108 are considered. In the summer of 2017, heat waves swept over a majority of area of NCP,
109 providing an excellent opportunity to investigate how the heat wave may have modulated BVOC
110 emissions and subsequent severe ozone events in NCP. Observation data and modeling are used
111 to delineate various factors contributing to enhanced biogenic emissions and elevated ozone
112 concentrations. More details of the data and model are provided in Methods.

113

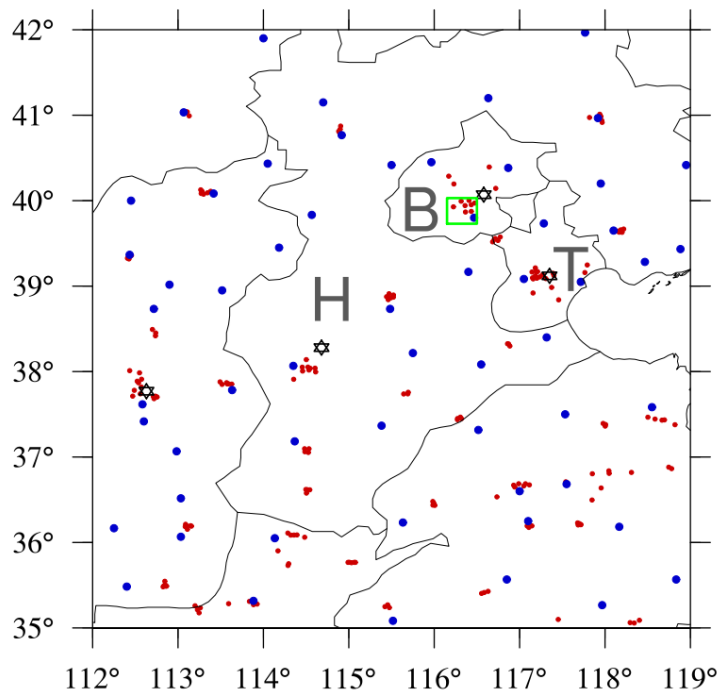
114

115

116

117 **2 Methods**

118 **Data and model configuration**



119
120 **Fig. 1** Distribution of observational sites over the NCP. (blue dots: daily maximum temperature daily
121 mean wind speed at 10-meter and daily total precipitation from China Meteorological Administration
122 (CMA); red dots: ozone monitoring sites from China National Environmental Monitoring Centre; black
123 hexagon: hourly temperature at 2-meter (T2), specific humidity at 2-meter (Q2), wind speed (WS10) and
124 direction (WD10) at 10-meter from MADIS; green box: urban area of Beijing). B, H, T represent Beijing,
125 Hebei Province and Tianjin, respectively.

126
127 The distribution of observed data was shown in Fig. 1. For instance, the meteorological
128 observations used in this study such as daily maximum temperature, daily mean wind speed, daily
129 total precipitation were obtained from the China Meteorological Data Service Center (CMA,
130 <http://data.cma.cn>), with blue dots shown in Fig. 1. Observed surface ozone data are obtained from
131 China National Environmental Monitoring Centre (<http://www.pm25.in>), with red dots shown in
132 Fig. 1. Meteorological Assimilation Data Ingest System (MADIS) hourly 2-meter temperature,
133 specific humidity, 10-meter wind speed and direction are available from The Meteorological

134 Assimilation Data Ingest System (MADIS; <https://madis.ncep.noaa.gov>), with hexagons shown in
135 Fig. 1.

136 For modeling the meteorological conditions, WRF V3.8.1 is used in this study. The domain is
137 centered at 110° E, 34° N, with a total of 34 vertical layers and top pressure at 50 hPa. The spatial
138 resolution is 36 km. The physics parameterizations used in this study are the same as our previous
139 studies (Gao et al., 2017; Zhang et al., 2019), including the Morrison double moment microphysics
140 (Morrison et al., 2009), the Rapid Radiative Transfer Model for GCMs (RRTMG) longwave and
141 shortwave radiation (Iacono et al., 2008; Morcrette et al., 2008), the unified Noah land surface
142 model (Chen and Dudhia, 2001), the Mellor-Yamada-Janjic planetary boundary layer (PBL)
143 scheme (Janjić, 1990, 1994; Mellor and Yamada, 1982), and the Grell-Freitas cumulus scheme
144 (Grell and Freitas, 2014). The initial and boundary conditions were generated from the NCEP
145 Climate Forecast System Reanalysis (CFSR) version 2 (Saha et al., 2013), with a spatial resolution
146 of 0.5°×0.5°.

147 For modeling atmospheric chemistry, the widely used Community Multi-scale Air Quality
148 (CMAQ) model (Byun and Ching, 1999; Byun and Schere, 2006), with the latest version 5.2, was
149 used in this study. The major gas phase chemistry was represented by the carbon-bond version 6
150 (CB06) and AERO6 aerosol module. Initial and boundary conditions were from Model for Ozone
151 and Related chemical Tracers, version 4 (MOZART-4) (Emmons et al., 2010). A dynamical
152 downscaling tool was developed in this study to link the Mozart output to CMAQ, based upon the
153 package of Mozart to WRF-Chem (mozbc: [https://www2.acom.ucar.edu/wrf-chem/wrf-chem-](https://www2.acom.ucar.edu/wrf-chem/wrf-chem-tools-community)
154 [tools-community](https://www2.acom.ucar.edu/wrf-chem/wrf-chem-tools-community)). With this tool, the default clean air profile provided by the CMAQ 5.2 package
155 was replaced by more realistic boundary variations at both the surface and different vertical levels.
156 A continuous run from June 1 to July 4 was performed, with the first week discarded as spinup.

157 The anthropogenic emissions of air pollutants in China were estimated by Tsinghua University,
158 detailed in previous studies (Wang et al., 2014; Zhao et al., 2013; 2017; 2018) and updated based
159 on the Multiresolution Emission Inventory for China (MEIC, 0.25°×0.25°;
160 <http://www.meicmodel.org/>) (Li et al., 2017a).

161 The biogenic emissions were calculated by the Model of Emissions of Gases and Aerosols
162 from Nature version 2.1 (MEGAN; Guenther et al., 2006; Guenther et al., 2012). MEGAN input
163 data includes three components: plant functional type (PFT), leaf area index (LAI) and emission
164 factors (EF). There is a total of 19 emission species including isoprene, terpenes, etc., derived

165 from more than 100 emissions compounds. For each of the 19 species, the emission rates F_i (μg
166 $\text{m}^{-2} \text{h}^{-1}$) for a certain grid were defined in Eq. 1 with i denoting the species.

$$167 \quad F_i = \gamma_i \sum \varepsilon_{i,j} \chi_j \quad (\text{Eq. 1})$$

168 where $\varepsilon_{i,j}$ and χ_j are the emission factor and fractional coverage of plant functional type (j) in
169 each grid respectively. γ_i is the emission activity defined based on light (denoted as L),
170 temperature (T), leaf age (LA), soil moisture (SM), leaf area index (LAI) and CO_2 inhibition
171 (denoted as CI), following Eq. 2.

$$172 \quad \gamma_i = C_{CE} LAI \gamma_{L,i} \gamma_{T,i} \gamma_{LA,i} \gamma_{SM,i} \gamma_{CI,i} \quad (\text{Eq. 2})$$

173 where C_{CE} is the canopy environment coefficient and 0.57 was used following Guenther et al.
174 (2012).

175 Compared with the previous version 2.0 with only 4 PFTs, there are 16 types of PFTs
176 represented in the new MEGAN version (Guenther et al., 2006; Guenther et al., 2012), allowing
177 for more accurate estimations of PFT-differentiated emission factors. PFT and LAI data were
178 from the MODIS MCD12Q1 (Friedl et al., 2010) and MCD15A2H datasets (Myneni et al., 2015)
179 respectively. The 8 vegetation types in MODIS were apportioned to the 16 PFT types in
180 MEGAN 2.1 based on the temperature zone. For example, MODIS has only one type of broad
181 leaf deciduous trees, while MEGAN 2.1 has three, including broad leaf deciduous tropical,
182 temperate and boreal trees. The broad leaf deciduous trees in MODIS are mapped onto the three
183 MEGAN types based on the latitudinal boundaries of the tropical, temperate and boreal zones,
184 with detailed mapping information provided in Table S4 in the supporting information. Monthly
185 mean LAIs were used in this study. The meteorological conditions used to generate biogenic
186 emission in MEGAN were provided by the WRF simulation.

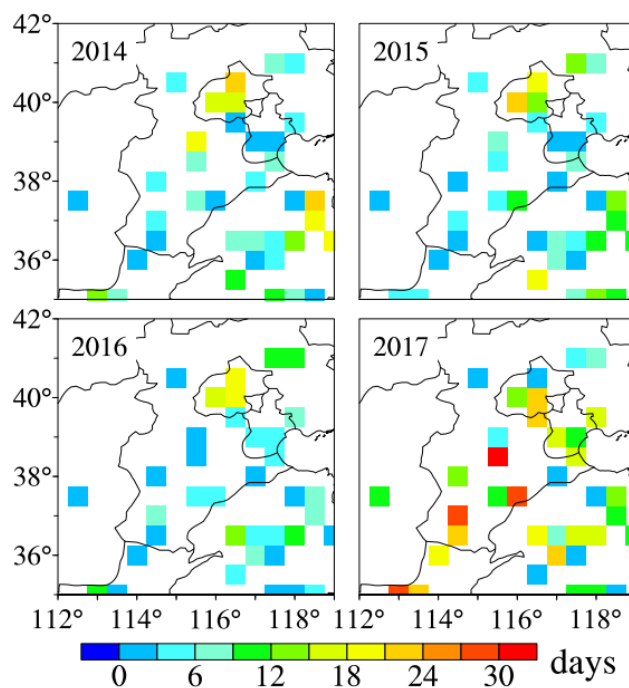
187

188 **3 Results**

189 **3.1 Observed ozone features**

190 The Technical Regulation on Ambient Air Quality Index (HJ633-2012) defines six classes of
191 ozone related pollution based on the daily maximum 8-h ozone concentration (MDA8). Classes I
192 and II are clean conditions (MDA8 less than 82 ppbv), class III (82-110 ppbv) indicates slight

193 pollution, class IV (110-135 ppbv) represents medium pollution, and classes V and VI are severe
 194 pollution conditions with MDA8 higher than 135 ppbv. Utilizing the observed MDA8 from
 195 China National Environmental Monitoring Centre (<http://www.pm25.in>), we first analyze the
 196 severe ozone pollution events considering their large impact on human health. The observed
 197 MDA8 was interpolated to a $0.5^\circ \times 0.5^\circ$ grid. Fig. 2 shows the number of severe ozone pollution
 198 days (MDA8 greater than 110 ppbv) during the summer of 2014-2017. The number of severe
 199 ozone pollution days in 2017 is larger than 9 in most areas, which is substantially higher than
 200 that of the other three years when most areas have fewer than 6 days. Frequent occurrence of
 201 severe ozone pollution happens in southern Beijing and south of Hebei Province (the area
 202 marked with letter H in Fig. 1).



203
 204 **Fig. 2** The number of severe ozone pollution days (MDA8 greater than 110 ppbv) during the
 205 summer of 2014-2017 over NCP.

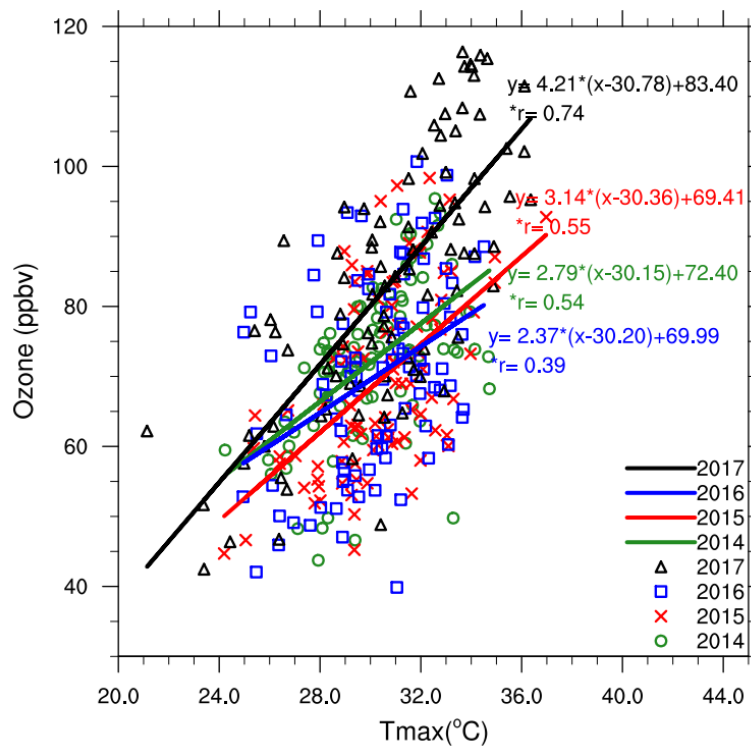
206
 207 **3.2 Meteorological factors modulating the high ozone events**

208 Correlation between MDA8 ozone and daily maximum 2-meter temperature (Fig. 3) shows
 209 statistically significant values for all four years, confirming the significant impact of temperature
 210 on ozone. However, the correlation in 2017 is obviously higher than the other three years, and
 211 the regression slope of $4.21 \text{ ppbv}/^\circ\text{C}$ is about 1.07 to $1.84 \text{ ppbv}/^\circ\text{C}$ higher than the other three

212 years, demonstrating the larger impact of temperature in 2017. Both the higher correlation (0.74)
 213 and the larger slope in 2017 are contributed mainly by days with ozone above the top 10% (104
 214 ppbv), which are related to the long-lasting high-ozone periods (see Table S1 and Fig. S1) during
 215 June 14-21 and June 26-July 3. Removing data above the top 10% brings the correlation (0.63)
 216 and slope closer to those of the other three years (Fig. S2). Furthermore, the mean temperature in
 217 2017 is not statistically different from that of the other three years, suggesting that the higher
 218 temperature period has disproportionate effects on ozone. Jaffe and Zhang (2017) also found a
 219 larger regression slope between ozone and temperature during the abnormally-warm month of
 220 June 2015 in the western U.S. compared to the previous five years with more normal
 221 temperatures.

222

223

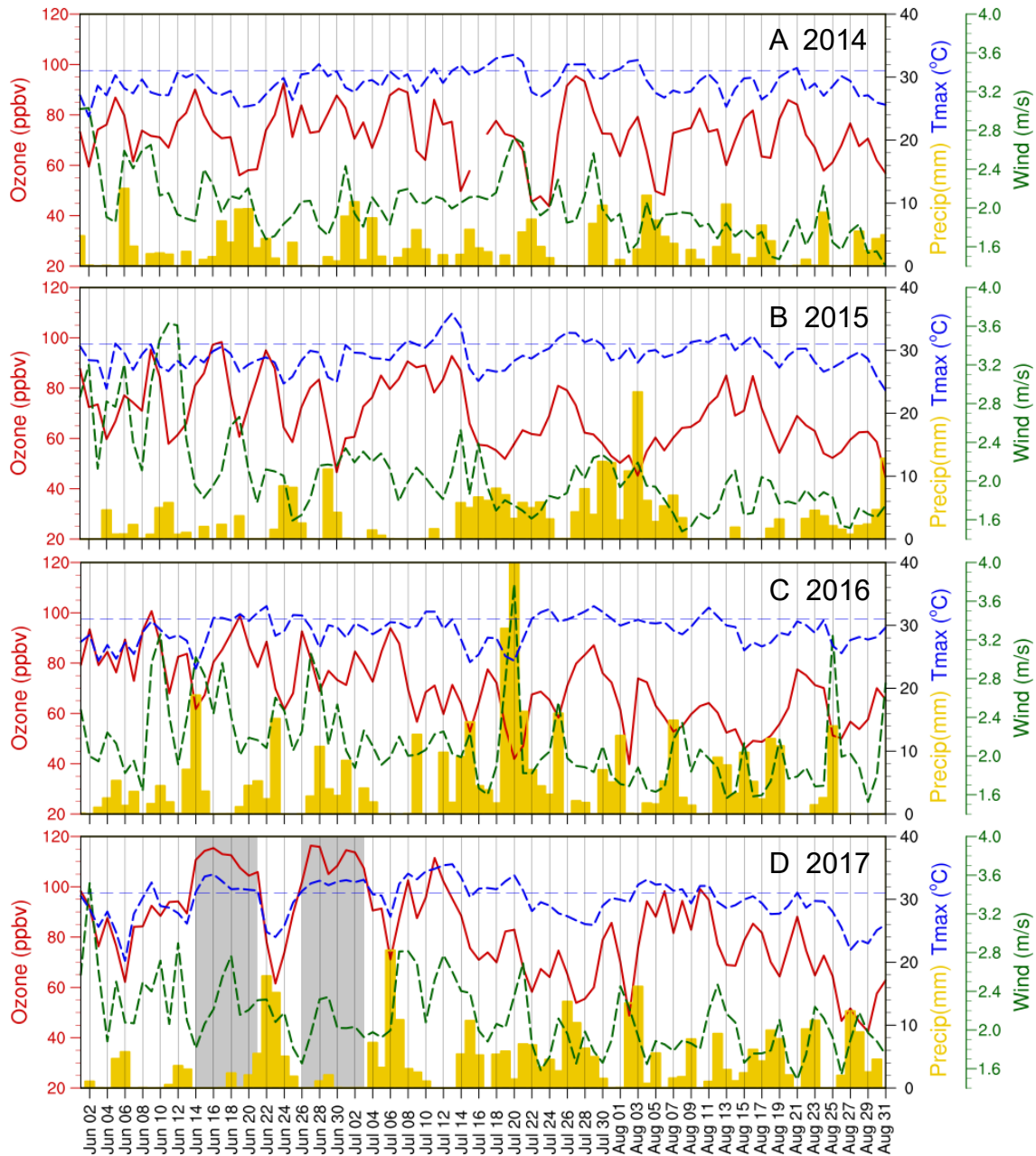


224

225 **Fig. 3** The correlation between summer MDA8 ozone and daily maximum 2-meter temperature (Tmax)
 226 for 2014-2017 over NCP. Regional mean was calculated from the observational sites over NCP so each
 227 data point corresponds to a regional mean value of MDA8.

228

229 To further delve into the meteorological factors modulating the ozone variations in the summer of
230 2014-2017, the time series of summer MDA8 ozone is shown in Fig. 4, along with daily maximum
231 temperature, wind speed and daily total precipitation. From Fig. 4D, the two long-lasting ozone
232 episodic events (event 1: June 14-21 and event 2: June 26-July 3) occur during heat waves
233 concomitant with stagnant (calm or low wind speed), dry (little or no precipitation) air and strong
234 solar radiation (not shown), conducive to ozone formation and accumulation. During the first three
235 days of these two high ozone episodic events, the regional mean daily maximum temperature is
236 32.3 °C, accounting for 90th percentile relative to a thirty-year period during 1987-2016. Moreover,
237 almost half of the stations with at least three continuous days exceeding their respective 95th
238 percentile from 1987-2016, satisfying the definitions of heat waves. This feature during the heat
239 wave period was illuminated in Table S2 as well, showing that among all the observational stations
240 with MDA8 ozone exceeding 110 ppbv, 87% (62%) and 96% (81%) occurs with daily precipitation
241 less than 1 mm (daily precipitation less than 1 mm and daily mean wind speed lower than 3 m/s).
242 Long lasting hot and stagnant weather conditions were not clearly observed during 2014-2016 (Fig.
243 4A-C).
244



245

246

247

248

249

250

251

252

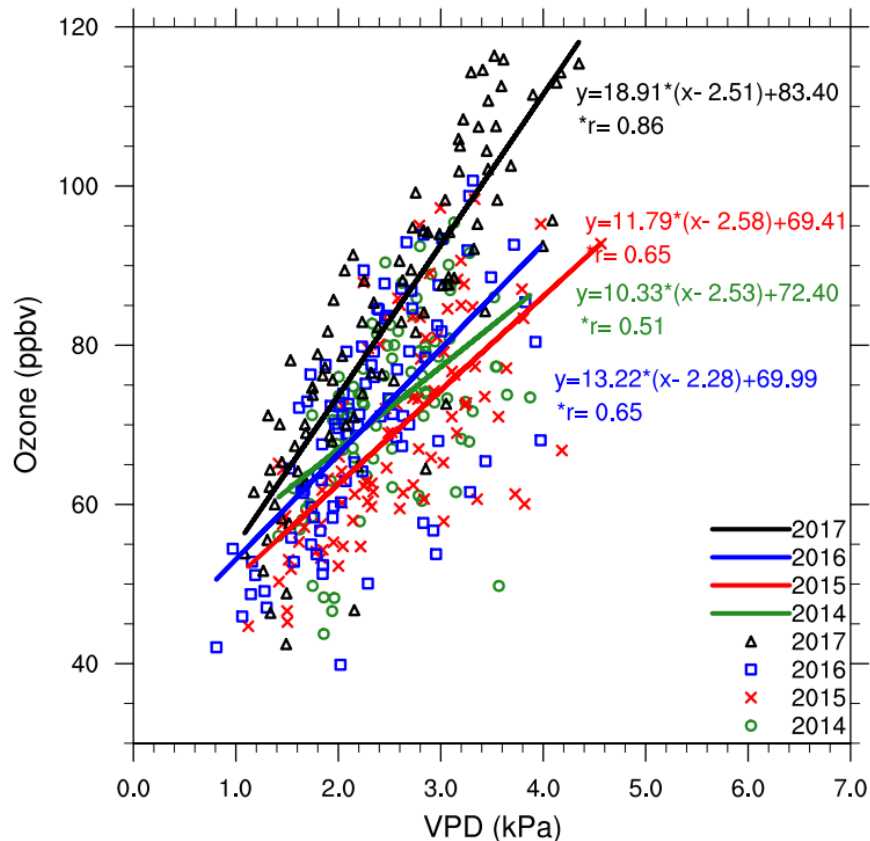
Fig. 4 Time series of observed MDA8 ozone (red lines; based on sites from China National Environmental Monitoring Centre; red points in Fig. 1), daily maximum temperature at 2m (blue lines), daily mean wind speed at 10m (green lines) and daily total precipitation (yellow bars) over NCP (based on sites from CMA; blue dots in Fig. 1) during the summer from 2014 to 2017. The regional precipitation was set to zero for a certain day if less than 15% (9 sites) of the total sites (58 sites) with daily total precipitation greater than 1 mm. The horizontal blue dash lines in each panel donate 31 °C.

253 **3.3 Effect of land use and biogenic emission on ozone**

254 Biogenic emissions contribute importantly to ozone formation. The MEGAN model has been
255 widely used to simulate biogenic emissions in air quality modeling studies (Guenther et al., 2012),
256 but recent research suggested that biogenic emissions may be underestimated in the model for
257 several reasons:

258 *a)* Water-stressed impact on biogenic emissions. Zhang and Wang (2016) found that two
259 high ozone events in the U.S. were associated with excess isoprene release due to dry and hot
260 weather conditions that induced water stress in plants. The increased vapor pressure deficit
261 (VPD; the pressure difference between saturation vapor and ambient vapor) drives the release of
262 more isoprene but the VPD effect on biogenic emissions has not been taken into consideration in
263 MEGAN 2.1, so the subsequent influence of biogenic emissions on ozone may be largely
264 underestimated. Zhang and Wang (2016) suggested a doubling of daily biogenic isoprene when
265 the daily VPD reaches 1.7 kPa or greater. It should be noted that this parameterization was based
266 upon the observed information over US, more tests may be needed in future when applying to
267 areas besides US. The monthly mean VPD spatial distribution in June 2017 (Fig. S3) as well as
268 the high correlation between observed MDA8 ozone and VPD (Fig. 5; with time series shown in
269 Fig. S4) suggests enhanced isoprene emission in NCP so we will test this VPD mechanism using
270 model simulations. Please note that in the latest version MEGAN 3 (Jiang et al., 2018), a new
271 approach was developed to quantify the drought effect on the isoprene emissions based on both
272 photosynthesis and water stress, yielding a general reduction of monthly mean isoprene emission
273 across the globe, including northern China. The impact of changes in isoprene emissions, based
274 on the new method, on ozone formation deserves further evaluation in future.

275

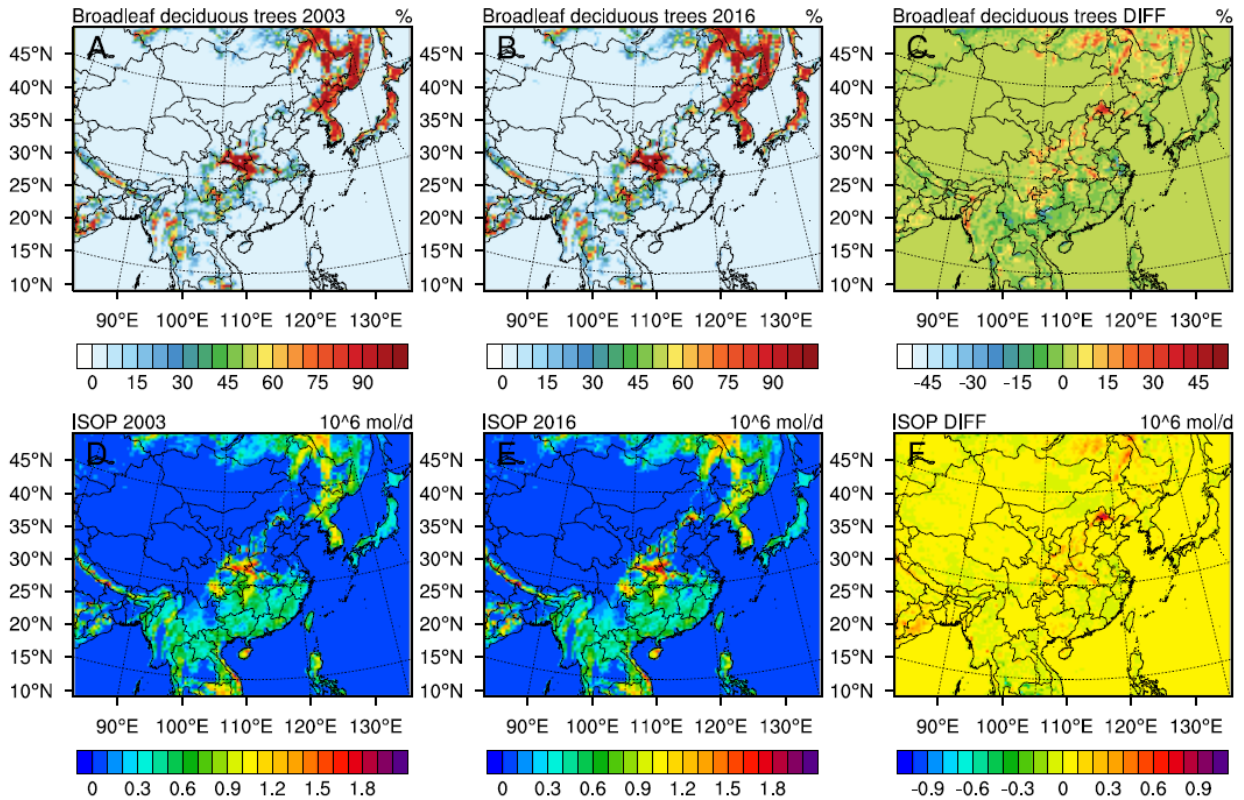


276

277 **Fig. 5** The correlation between summer MDA8 ozone and daily maximum VPD during 2014-2017
 278 over NCP. Regional mean was calculated from the observational sites over NCP so each data point
 279 corresponds to a regional mean value of MDA8.

280 *b)* Changes in land cover may affect biogenic emissions. As reflected by the much higher
 281 emission factor, biogenic isoprene emission is enhanced in broad leaf forest relative to other land
 282 cover types such as needle leaf forest, shrub, grass or crop (Table 2 in Guenther et al. (2012)). In
 283 NCP, broad leaf tree is the dominant land cover type and its coverage has been increasing
 284 dramatically since the 1970s, primarily a result of the “Three-North Protection Forest System”
 285 project. For example, based on Moderate Resolution Imagine Spectroradiometer (MODIS) land
 286 use data (Friedl et al., 2010), the coverage of broadleaf deciduous temperate tree nearly doubled
 287 from 2003 to 2016 over NCP (top row of Fig. 6). This has resulted in a substantial increase of
 288 isoprene emissions between 2003 and 2016 (Fig. 6), particularly north of the Beijing, Hebei and
 289 Tianjin, where the increase is more than 200%. Combining the point *a)* described above, the
 290 underestimation of biogenic emission due to changes in land cover may be exaggerated in years
 291 with high temperatures and high VPD. It is vital to quantify the effect of land cover changes on

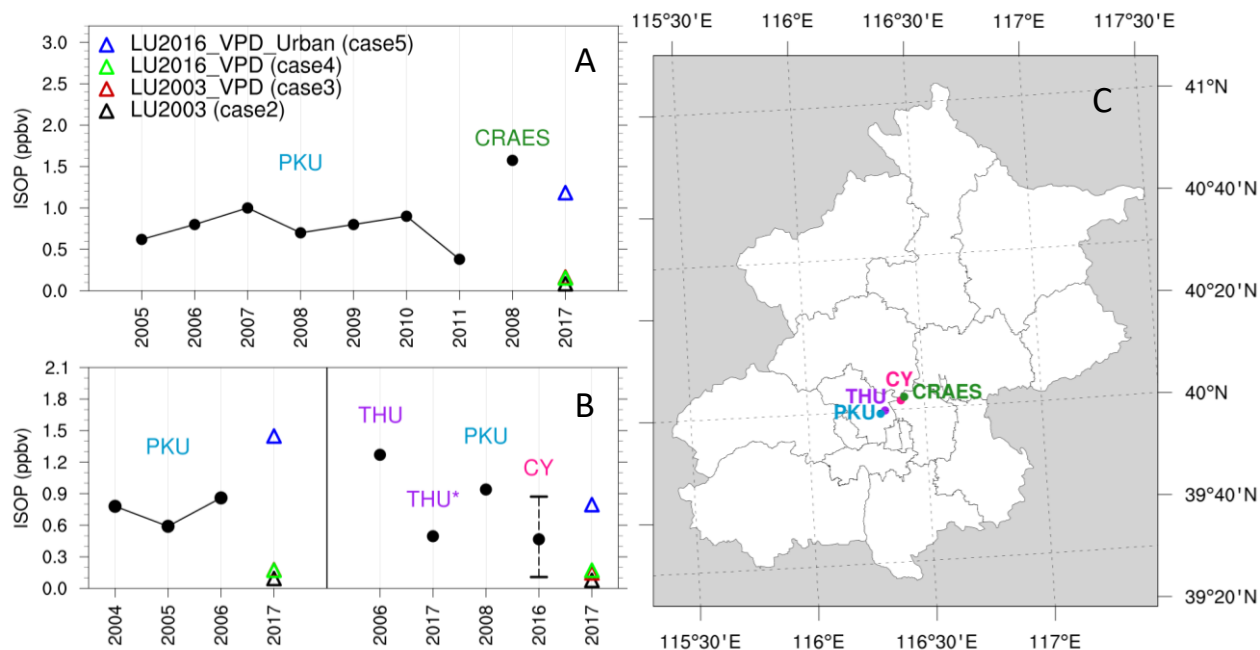
292 biogenic emissions such as isoprene and the subsequent impact on ozone formation.



293
294 **Fig. 6** Spatial distribution of broadleaf deciduous trees in 2003 (Fig. 6A), 2016 (Fig. 6B) and their
295 differences (2016-2003; Fig. 6C), and the biogenic isoprene emissions during the heat waves periods (June
296 14-21 2017; June 26-July 3 2017) based on the land cover in 2003 (Fig. 6D), 2016 (Fig. 6E) and their
297 differences (2016-2003; Fig. 6F).

298 c) Impact of urban landscape on biogenic emission. Land use type cataloged in the MODIS
299 MCD12Q1 product (Friedl et al., 2010) does not take into consideration urban green spaces, which
300 may lead to a 15% underestimation of total BVOC emissions in 2015 over Beijing (Ren et al.,
301 2017). Generally, urban ozone production is highly sensitive to VOCs emissions (Xing et al., 2011;
302 Liu et al., 2012). Bell and Ellis (2004) found a doubling of ozone in urban area relative to rural
303 areas for the same percentage increase of biogenic emissions. The impact of biogenic emission
304 from urban landscape on urban ozone formation has not been considered in previous studies. For
305 sensitivity analysis, we added a 15% increase of the total BVOCs emissions in Beijing to
306 investigate its impact on urban ozone formation. These emissions were distributed evenly in the
307 urban core area of Beijing as the increase of biogenic emissions from urban landscape were only
308 available for Beijing.

309 To elucidate the mechanism modulating the ozone events discussed above, the regional
310 meteorology and air quality model WRF/CMAQ was used to conduct simulations during June 8
311 to July 4 2017. The WRF simulations generally meet the benchmark standard for meteorological
312 variables (Table S3). For air quality simulations, five scenarios were designed, with biogenic
313 emissions ignored in the base case. Compared to the base case, case 2 adds biogenic emission
314 associated with the land cover of 2003, and cases 3, 4 and 5 are the same as case 2 except for the
315 inclusion of the VPD effect, both VPD and land cover of 2016, and VPD and land cover of 2016
316 combined with the effect of urban green spaces, respectively. To validate the reasonableness of
317 adding the biogenic emission, we first evaluate the simulated isoprene concentration, one of the
318 most important species closely related to ozone formation, from WRF/CMAQ among different
319 cases. Since there is a lack of observed ambient isoprene concentration during this study period,
320 the data available (mostly over Beijing) from the literature was retrieved and used as cross
321 comparison with the model results (Fig. 7). From Fig. 7A,B, the observed mean isoprene
322 concentration ranges from 0.4 ppbv to 1.6 ppbv in various sites of Beijing. The model simulations
323 by taking into consideration of isoprene emissions from VPD, land cover of 2016 and urban green
324 spaces (case 5) yield the best performance, with isoprene concentration of 0.8 ppbv to 1.4 ppbv.
325 However, the other cases (with isoprene concentrations of 0.1 ppbv to 0.2 ppbv) substantially
326 underestimate the isoprene concentrations. Therefore, the isoprene emissions from urban green
327 spaces (comparing case 5 and case 4) in Beijing plays a vital role in the isoprene concentrations,
328 which subsequently affect the ozone formation which will be further evaluated and discussed
329 below.



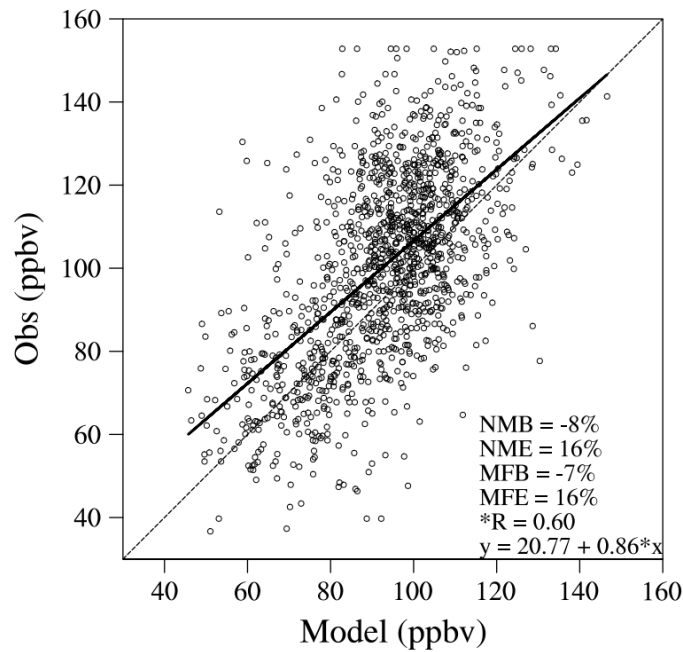
330

331 **Fig. 7** The comparison of isoprene concentrations between model simulations and observations in Beijing.
 332 The black dots represent the observed data from various of literatures, whereas the hollow triangles (in
 333 black, red, green and blue) represent the model simulations for the four cases described above (cases 2-5).
 334 For each observational dataset, the corresponding reference number was labelled on the right of the site
 335 name in Fig. 7A,B, with site locations shown in Fig. 7C. One exception is the unpublished work in THU*
 336 which is from the observations using proton-transfer-reaction time-of-flight mass spectrometer (PTR-ToF-
 337 MS) conducted by Tsinghua University (manuscript in preparation). Please note that no observation period
 338 matches exactly our simulation time, making the comparison more qualitative rather than quantitative.
 339 However, the model evaluation did match the respective location and time (i.e., day-time or selected hour)
 340 among different observations. The model simulation period used in the comparison is from June 8 to July
 341 4, 2017. For observations, in Fig. 7A, the dots represent the mean isoprene concentrations during day-time
 342 in August from 2005 to 2011 at Peking University (PKU; (Zhang et al., 2014); left of Fig. 7A) and from 16
 343 July to 18 August 2008 at Chinese Research Academy of Environmental Science (CRAES; (Yang et al.,
 344 2018); right of Fig. 7A). In Fig. 7B, the dots on the left represent the mean isoprene concentration of hour
 345 8:00 and hour16:00 (local standard time) in August from 2004-2006 (with detailed measurement time
 346 shown in Table 1 of (Shao et al., 2009)) in PKU. The observational data on the right of Fig. 7B is on daily
 347 mean scale during a certain period (with one site of CY showing minimal and maximal daily mean values
 348 during the period) from four sources. The two leftmost dots are located at the campus of Tsinghua
 349 University (THU), with one from August 15-20 2006 (Duan et al., 2008) and the other from July 14 to
 350 August 5 2017 (manuscript in preparation as explained above). The third dot represents data measured at
 351 PKU from July 24 to August 27, 2008 (Liu et al., 2015) and the fourth dot indicates data observed at
 352 Chaoyang District (CY; (Gu et al., 2019)).

353

354 Since the effect of urban landscape was only applied to Beijing in case 5, we use case 4
 355 (combination of VPD and land cover change effects) (referred to as B_MDA8) as the reference.

356 Therefore, we first compare MDA8 ozone in case 4 with observations. To facilitate the comparison,
 357 observational data was interpolated to the model grids and reasonable performance is achieved
 358 with MFB/MFE of -7%/16% (Fig. 8). Considering the mean bias likely attributed to the factors
 359 such as emission uncertainty or model inherent biases, thus a bias correction was applied to each
 360 case by adding 7% of mean observed MDA8 ozone during June 8-July 4 2017.



361
 362 **Fig. 8** MDA8 ozone evaluation over NCP during June 8 to July 4 in 2017. NMB, NME, MFB, MFE
 363 represent normalized mean bias, normalized mean error, mean fractional bias and mean fractional error,
 364 respectively.

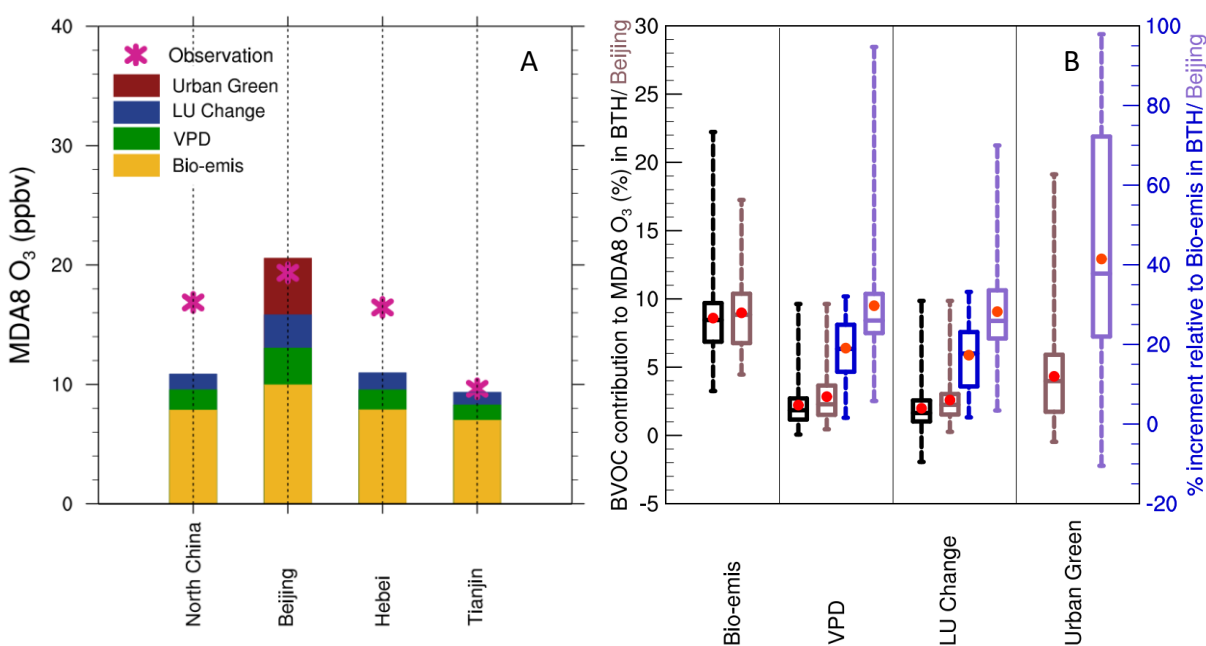
365 Zooming into the two ozone episodic events (June 14-21, June 26-July 3), the mean MDA8
 366 values of case 4 are 98.02 ppbv, 108.89 ppbv, 95.75 ppbv, and 98.98 ppbv for NCP, Beijing, Hebei
 367 and Tianjin, respectively, during the heat wave periods (June 14-21, 2017; June 26-July 3, 2017),
 368 whereas the MDA8 ozone value for the case (case 1) without biogenic emission are 87.15 ppbv,
 369 93.06 ppbv, 84.78 ppbv and 89.65 ppbv for the corresponding region. The ozone increment from
 370 case 2 to case 5 (as well as observations; magenta stars in Fig. 9A) relative to case 1 was shown in
 371 Fig. 9A for these regions. Including biogenic emission based on the land cover of 2003 (case 2)
 372 yields an extra mean MDA8 ozone of 7.84 ppbv (8% of B_MDA8), 9.96 ppbv (9% of B_MDA8),
 373 7.86 ppbv (8% of B_MDA8) and 6.99 ppbv (7% of B_MDA8) for NCP, Beijing, Hebei and Tianjin,
 374 respectively (yellow bars in Fig. 9A), compared to case 1. Including the VPD effect (case 3) adds

375 an extra mean MDA8 of 1.71 ppbv in NCP compared to case 2, and the enhancement is highest in
376 Beijing (3.08 ppbv) (green bars in Fig. 9A). Additional MDA8 ozone enhancement is simulated
377 by including the effect of land cover change (increase in natural broadleaf forest; top row in Fig.
378 6; case 4), i.e., an extra MDA8 of 1.32 ppbv in NCP relative to case 3, with the highest contribution
379 of 2.79 ppbv in Beijing (blue bars in Fig. 9A). The urban landscape (case 5) in Beijing yields an
380 extra 4.74 ppbv or 4% of MDA8 compared to case 4, almost doubling the effect of VPD and land
381 cover change in Beijing. The larger percentage increase in MDA8 ozone (41% from Fig. 9A, which
382 will be discussed in Fig. 9B as well) due to urban landscape relative to the prescribed 15% increase
383 in BVOC emission in Beijing supports the notion of an amplified MDA8 ozone response in urban
384 areas because of the high sensitivity of ozone to VOCs emissions, which well matches
385 observational data (magenta star).

386 To further illustrate the contributions of BVOC to MDA8, Fig. 9B shows the contribution of
387 biogenic emissions (Bio_emis, based on land cover of 2003), VPD, land cover change, and urban
388 landscape (or urban green) to MDA8 as a fraction of the MDA8 of B_MDA8 (left y-axis in Fig.
389 9B) and as percentage increment relative to the MDA8 contributed by biogenic emissions in case
390 2 (right y-axis in Fig. 9B) in BTH (Beijing, Tianjin, Hebei; with letters B, T and H marked in Fig.
391 1) and Beijing. For BTH, the mean contribution to B_MDA8 is 9%, 2% and 2% for Bio_emis,
392 VPD and land cover change (red dots in the black bars in Fig. 9B), respectively, with maximum
393 contributions of 22%, 10% and 10%. For Beijing, the contributions of Bio_emis, VPD, land cover
394 change, and urban landscape are 9%, 3%, 3% and 4% respectively (red dots in the brown bars in
395 Fig. 9B). Urban landscape (19%) contributes more than Bio_emis (17%) in the urban area of
396 Beijing in terms of the maximal contribution (maximum value of the brown box in Fig. 9B).
397 Compared with Bio_emis, the mean increments are 19% and 17% for VPD and land cover change
398 (red dots in the blue bars in Fig. 9B). For Beijing, the mean additional enhancements are 30%, 28%
399 and 41% for VPD, land cover change and urban landscape relative to Bio_emis (red dots in the
400 purple bars in Fig. 9B), with a combined increment of 99% compared to the MDA8 ozone
401 contributed by biogenic emission based on the land cover of 2003. Although only grid cells with
402 both simulations and observations available are used in Fig. 9B, the results are similar if all model
403 grids points were used (not shown).

404 In order to demonstrate whether changes of land cover and VPD play any roles during normal
 405 ozone conditions, we conducted another sets of simulations (the same as cases 2-4 discussed above)
 406 during June 8 to mid-July in 2016, similar period as 2017. The mean MDA8 ozone concentrations
 407 over NCP during this entire period in 2017 for case 2 is 79.03 ppbv, and statistical significant
 408 enhancement (1.34 ppbv) was achieved in case 3. In comparison to case 3, the land cover change
 409 in case 4 shows statistical significant increase as well (1.13 ppbv). As expected, looking at the
 410 entire period in 2016 (June 8-July 4), statistical significant, and even higher in relative to 2016,
 411 increase was achieved in case 3 (1.55 ppbv) compared to case 2 (90.11 ppbv), and case 4 (1.23
 412 ppbv) compared to case 3. Therefore, the land cover and VPD may be applied in both episodic
 413 events and conditions with normal ozone concentrations.

414

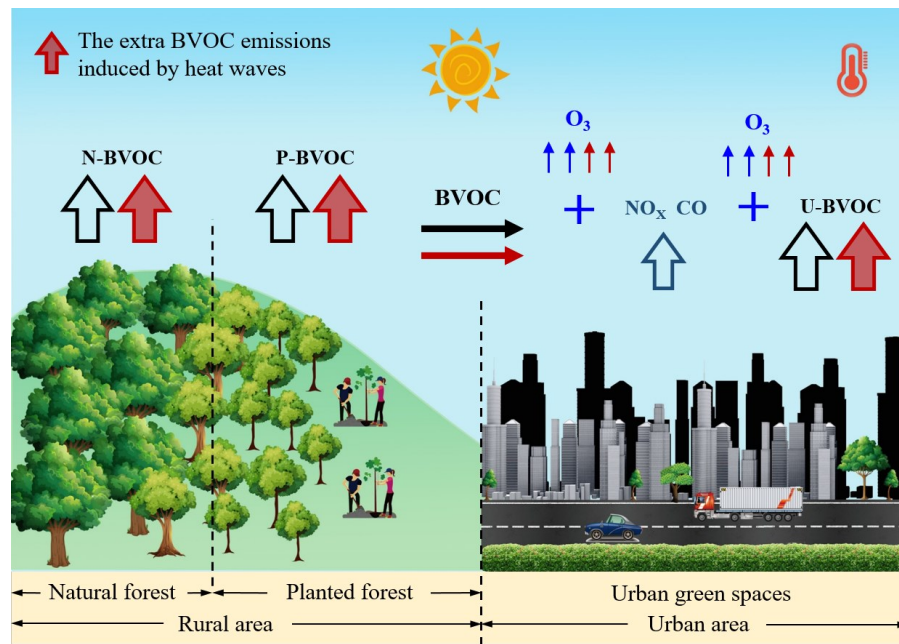


415
 416 **Fig. 9** Biogenic contribution to MDA8 ozone during the heat wave periods (June 14-21; June 26-July 3),
 417 shown by the individual (left) and percentage contribution (right) of standard biogenic emissions using
 418 MEGAN 2.1 with the land cover of 2003 (Bio-emis), VPD effect, land cover (LC) change and urban green
 419 spaces. The color bars (Fig. 9A) represent the simulated contributions of biogenic emissions (yellow), VPD
 420 (green), land use changes (blue), and urban green (red) to the MDA8 ozone concentrations in NCP, Beijing,
 421 Hebei and Tianjin respectively. The magenta stars in Fig. 9A represent the observed biogenic emissions
 422 calculated by subtracting the contribution to MDA8 ozone simulated in the base case from the observed

423 total MDA8 ozone. The box-and-whisker plot shows the contribution of biogenic emissions, VPD, land
 424 cover change and urban green spaces to the total MDA8 ozone in BTH (black) and Beijing (brown) (y-axis
 425 on the left), and the percentage increment (right y-axis) of VPD, land cover change and urban green relative
 426 to MDA8 induced by Bio-emis for BTH (blue) and Beijing (purple). Please note that urban green spaces
 427 are only available for Beijing. The top and bottom edges of the boxes represent the 75 and 25 percentiles,
 428 with the centered line and red dot showing the median and mean, respectively.

429 Herein the mechanisms for ozone enhancement are summarized in the schematic of Fig. 10.
 430 Both natural and anthropogenic emissions contribute to ozone formation. Because of the “Three-
 431 North Protection Forest System” project, natural forest north of Beijing has more than tripled in
 432 area coverage compared to 2003, leading to an increasing trend in biogenic emissions. Under heat
 433 wave conditions, biogenic emissions may be further enhanced through the effect of VPD in
 434 addition to the effect of temperature. For urban areas, even more biogenic emissions may be
 435 emitted from urban landscape. All these mechanisms for increasing biogenic emissions could
 436 enhance ozone formation, particularly over urban areas such as Beijing.

437



438

439 **Fig. 10** A schematic diagram of the impact of biogenic emission on ozone formation. N-BVOC refers to
 440 natural biogenic emission, P-BVOC refers to the biogenic emission from planted forest and in this study

441 representing the increase of forest coverage. U-BVOC refers to urban BVOC generated from urban green
442 spaces. The red thick upward arrows indicate extra VOCs may be induced by the heat waves.

443

444 **4 Discussion**

445 The mechanisms contributing to the severe ozone pollution events in the summer of 2017 in
446 NCP were investigated. Two severe tropospheric ozone pollution events occurred in the NCP
447 during the periods of June 14 to 21 and June 26 to July 3. We provided support for the roles of
448 the observed meteorological conditions including high temperature and stagnant dry weather,
449 which favor high ozone concentrations. More importantly, the influence of biogenic emissions
450 on ozone formation was investigated in more detail by incorporating important biogenic
451 emission factors that are typically ignored in regional model simulations. Biogenic emissions
452 based on the land cover of 2003 yields an extra mean MDA8 ozone of 7.84 ppbv for the NCP.
453 Including the VPD effect and land cover change adds 1.71 ppbv and 1.32 ppbv of ozone in the
454 NCP. These contributions are even larger in Beijing, with VPD adding 3.08 ppbv and land cover
455 change adding 2.79 ppbv. Most notably, biogenic emissions from urban landscape (i.e., green
456 spaces) have so far not been considered in ozone regional modeling studies to our knowledge. By
457 adding this source in the urban area of Beijing, substantial ozone enhancement was simulated,
458 bringing the WRF/CMAQ simulation of MDA8 closer to observations. The urban landscape in
459 Beijing yields an extra 4.74 ppbv of MDA8, comparable to the combined effect of VPD and land
460 cover change in Beijing. Together, the combined effect of VPD, land cover change, and urban
461 landscape doubles the effect of biogenic emission calculated based on the land cover of 2003 and
462 not including the VPD and urban landscape effects. Please note that although the urban isoprene
463 emission from landscape in Beijing only accounts for 15% (Ren et al., 2017), the location of the
464 emissions may play a much larger role in contributing to the urban isoprene concentration. As
465 was shown in Fig. 6, most of the isoprene emissions from the forest in Beijing is located in the
466 rural area, which is relatively far from the urban area. Considering the short lifetime of isoprene,
467 it may not be as efficient as the urban isoprene emission resulting from urban landscape directly
468 in modulating the isoprene concentrations. Therefore, the urban isoprene emission may play
469 much more significant role in urban photochemical reactions compared to the isoprene emissions
470 from the forest over the rural areas.

471 The BVOC emissions from urban green spaces are projected to increase by more than two
472 times in 2050 due to urban area expansion (Ren et al., 2017). Together with the more frequent heat
473 waves projected for the future (Gao et al., 2012; Zhang et al., 2018), the impact of biogenic
474 emissions on ozone pollution in the NCP will likely play an increasingly important role in ozone
475 pollution and should be taken into considerations in future air quality management plans to address
476 issues of air quality and health. The effect of urban green spaces was only considered in Beijing
477 in this study as we lack the data to parameterize this effect in other regions. Considering the
478 substantial effect of urban green spaces on urban ozone formation, it is vital to evaluate similar
479 effects in other cities where ozone pollution is a concern.

480

481 **Competing interests.** The authors declare that they have no conflict of interest.

482 **Acknowledgement.** This research was supported by grants from the National Key Project
483 of MOST (2017YFC1404101), National Natural Science Foundation of China (41705124,
484 21625701, 41722501, 91544212), Shandong Provincial Natural Science Foundation, China
485 (ZR2017MD026) and Fundamental Research Funds for the Central Universities (201941006,
486 201712006). Y. Wang was supported by the National Science Foundation Atmospheric
487 Chemistry Program. PNNL is operated for DOE by Battelle Memorial Institute under contract
488 DE-AC05-76RL01830.

489

490 **Author contributions.** YG came up with the original idea and YG, YW and CL designed the
491 research. MM conducted all the analysis, SZ, LRL, SW, BZ, XC, HS, TZ, LS, XY and HW
492 wrote the paper.

493 **References:**

- 494 Avnery, S., Mauzerall, D. L., Liu, J. F., and Horowitz, L. W.: Global crop yield reductions due to
495 surface ozone exposure: 1. Year 2000 crop production losses and economic damage, *Atmos*
496 *Environ*, 45, 2284-2296, 10.1016/j.atmosenv.2010.11.045, 2011.
- 497 Bell, M., and Ellis, H.: Sensitivity analysis of tropospheric ozone to modified biogenic emissions
498 for the Mid-Atlantic region, *Atmos Environ*, 38, 1879-1889, 2004.

- 499 Byun, D., and Ching, J. K. S.: Science Algorithms of the EPA Models-3 CommunityMultiscale
500 Air Quality (CMAQ) Modeling System., U. S. Environmental Protection Agency, Office of
501 Research and Development, EPA, Washington, DC, 727, 1999.
- 502 Byun, D., and Schere, K. L.: Review of the governing equations, computational algorithms, and
503 other components of the models-3 Community Multiscale Air Quality (CMAQ) modeling
504 system, *Appl Mech Rev*, 59, 51-77, 10.1115/1.2128636, 2006.
- 505 Chen, F., and Dudhia, J.: Coupling an advanced land surface-hydrology model with the Penn
506 State-NCAR MM5 modeling system. Part I: Model implementation and sensitivity, *Mon*
507 *Weather Rev*, 129, 569-585, 10.1175/1520-0493(2001)129<0569:caalsh>2.0.co;2, 2001.
- 508 Chen, L., Guo, B., Huang, J. S., He, J., Wang, H. F., Zhang, S. Y., and Chen, S. X.: Assessing
509 air-quality in Beijing-Tianjin-Hebei region: The method and mixed tales of PM_{2.5} and O₃, *Atmos*
510 *Environ*, 193, 290-301, 2018a.
- 511 Chen, W. H., Guenther, A. B., Wang, X. M., Chen, Y. H., Gu, D. S., Chang, M., Zhou, S. Z.,
512 Wu, L. L., and Zhang, Y. Q.: Regional to global biogenic isoprene emission responses to
513 changes in vegetation from 2000 to 2015, *J Geophys Res-Atmos*, 123, 3757-3771,
514 10.1002/2017jd027934, 2018b.
- 515 Chen, Z., Zhuang, Y., Xie, X., Chen, D., Cheng, N., Yang, L., and Li, R.: Understanding long-
516 term variations of meteorological influences on ground ozone concentrations in Beijing during
517 2006-2016, *Environ Pollut*, 245, 29-37, 10.1016/j.envpol.2018.10.117, 2019.
- 518 Cheng, Y. F., Zheng, G. J., Wei, C., Mu, Q., Zheng, B., Wang, Z. B., Gao, M., Zhang, Q., He, K.
519 B., Carmichael, G., Poschl, U., and Su, H.: Reactive nitrogen chemistry in aerosol water as a
520 source of sulfate during haze events in China, *Sci Adv*, 2, 2016.
- 521 Duan, J. C., Tan, J. H., Yang, L., Wu, S., and Hao, J. M.: Concentration, sources and ozone
522 formation potential of volatile organic compounds (VOCs) during ozone episode in Beijing,
523 *Atmos Res*, 88, 25-35, 2008.
- 524 Emberson, L. D., Buker, P., Ashmore, M. R., Mills, G., Jackson, L. S., Agrawal, M.,
525 Atikuzzaman, M. D., Cinderby, S., Engardt, M., Jamir, C., Kobayashi, K., Oanh, N. T. K.,
526 Quadir, Q. F., and Wahid, A.: A comparison of North American and Asian exposure-response
527 data for ozone effects on crop yields, *Atmos Environ*, 43, 1945-1953,
528 10.1016/j.atmosenv.2009.01.005, 2009.
- 529 Emmons, L. K., et al.: Description and evaluation of the Model for Ozone and Related chemical
530 Tracers, version 4 (MOZART-4), *Geosci Model Dev*, 3, 43-67, 10.5194/gmd-3-43-2010, 2010.

531 Fiore, A. M., Naik, V., and Leibensperger, E. M.: Air quality and climate connections, *J Air*
532 *Waste Manage*, 65, 645-685, 10.1080/10962247.2015.1040526, 2015.

533 Friedl, M. A., Sulla-Menashe, D., Tan, B., Schneider, A., Ramankutty, N., Sibley, A., and
534 Huang, X. M.: MODIS Collection 5 global land cover: Algorithm refinements and
535 characterization of new datasets, *Remote Sens Environ*, 114, 168-182, 2010.

536 Fu, J. S., Dong, X., Gao, Y., Wong, D. C., and Lam, Y. F.: Sensitivity and linearity analysis of
537 ozone in East Asia: The effects of domestic emission and intercontinental transport, *J Air Waste*
538 *Manage*, 62, 1102-1114, 2012.

539 Fu, Y., and Liao, H.: Impacts of land use and land cover changes on biogenic emissions of
540 volatile organic compounds in China from the late 1980s to the mid-2000s: Implications for
541 tropospheric ozone and secondary organic aerosol, *Tellus B*, 66, ARTN 24987
542 10.3402/tellusb.v66.24987, 2014.

543 Gao, Y., Fu, J. S., Drake, J. B., Liu, Y., and Lamarque, J. F.: Projected changes of extreme
544 weather events in the eastern United States based on a high resolution climate modeling system,
545 *Environ Res Lett*, 7, 2012.

546 Gao, Y., Fu, J. S., Drake, J. B., Lamarque, J. F., and Liu, Y.: The impact of emission and climate
547 change on ozone in the United States under representative concentration pathways (RCPs),
548 *Atmos Chem Phys*, 13, 9607-9621, 10.5194/acp-13-9607-2013, 2013.

549 Gao, Y., Leung, L. R., Zhao, C., and Hagos, S.: Sensitivity of US summer precipitation to model
550 resolution and convective parameterizations across gray zone resolutions, *J Geophys Res-Atmos*,
551 122, 2714-2733, 2017.

552 Ghirardo, A., Xie, J. F., Zheng, X. H., Wang, Y. S., Grote, R., Block, K., Wildt, J., Mentel, T.,
553 Kiendler-Scharr, A., Hallquist, M., Butterbach-Bahl, K., and Schnitzler, J. P.: Urban stress-
554 induced biogenic VOC emissions and SOA-forming potentials in Beijing, *Atmos Chem Phys*,
555 16, 2901-2920, 10.5194/acp-16-2901-2016, 2016.

556 Grell, G. A., and Freitas, S. R.: A scale and aerosol aware stochastic convective parameterization
557 for weather and air quality modeling, *Atmos Chem Phys*, 14, 5233-5250, 10.5194/acp-14-5233-
558 2014, 2014.

559 Gu, Y. Y., Li, Q. Q., Wei, D., Gao, L. R., Tan, L., Su, G. J., Liu, G. R., Liu, W. B., Li, C. Q., and
560 Wang, Q. L.: Emission characteristics of 99 NMVOCs in different seasonal days and the
561 relationship with air quality parameters in Beijing, China, *Ecotox Environ Safe*, 169, 797-806,
562 2019.

563 Guenther, A., Karl, T., Harley, P., Wiedinmyer, C., Palmer, P. I., and Geron, C.: Estimates of
564 global terrestrial isoprene emissions using MEGAN (Model of Emissions of Gases and Aerosols
565 from Nature), *Atmos Chem Phys*, 6, 3181-3210, DOI 10.5194/acp-6-3181-2006, 2006.

566 Guenther, A. B., Jiang, X., Heald, C. L., Sakulyanontvittaya, T., Duhl, T., Emmons, L. K., and
567 Wang, X.: The Model of Emissions of Gases and Aerosols from Nature version 2.1
568 (MEGAN2.1): An extended and updated framework for modeling biogenic emissions, *Geosci
569 Model Dev*, 5, 1471-1492, 2012.

570 Han, X., Zhu, L. Y., Wang, S. L., Meng, X. Y., Zhang, M. G., and Hu, J.: Modeling study of
571 impacts on surface ozone of regional transport and emissions reductions over North China Plain
572 in summer 2015, *Atmos Chem Phys*, 18, 12207-12221, 2018.

573 Iacono, M. J., Delamere, J. S., Mlawer, E. J., Shephard, M. W., Clough, S. A., and Collins, W.
574 D.: Radiative forcing by long-lived greenhouse gases: Calculations with the AER radiative
575 transfer models, *J Geophys Res-Atmos*, 113, D13103, 10.1029/2008jd009944, 2008.

576 Jacob, D. J., and Winner, D. A.: Effect of climate change on air quality, *Atmos Environ*, 43, 51-
577 63, 10.1016/j.atmosenv.2008.09.051, 2009.

578 Jaffe, D. A., and Zhang, L.: Meteorological anomalies lead to elevated O₃ in the western U. S. in
579 June 2015, *Geophys Res Lett*, 44, 1990-1997, 2017.

580 Janjić, Z. I.: The step-mountain coordinate: Physical package, *Mon Weather Rev*, 118, 1429-
581 1443, 10.1175/1520-0493(1990)118<1429:tsmcpp>2.0.co;2, 1990.

582 Janjić, Z. I.: The Step-Mountain Eta Coordinate Model: Further developments of the convection,
583 viscous sublayer, and turbulence closure schemes, *Mon Weather Rev*, 122, 927-945,
584 10.1175/1520-0493(1994)122<0927:TSMECM>2.0.CO;2, 1994.

585 Jiang, X. Y., Guenther, A., Potosnak, M., Geron, C., Seco, R., Karl, T., Kim, S., Gu, L. H., and
586 Pallardy, S.: Isoprene emission response to drought and the impact on global atmospheric
587 chemistry (vol 183, pg 69, 2018), *Atmos Environ*, 185, 272-273, 2018.

588 Li, K., Jacob, D. J., Liao, H., Shen, L., Zhang, Q., and Bates, K. H.: Anthropogenic drivers of
589 2013-2017 trends in summer surface ozone in China, *Proc Natl Acad Sci USA*,
590 10.1073/pnas.1812168116, 2019.

591 Li, M., et al.: MIX: A mosaic Asian anthropogenic emission inventory under the international
592 collaboration framework of the MICS-Asia and HTAP, *Atmos Chem Phys*, 17, 935-963,
593 10.5194/acp-17-935-2017, 2017a.

- 594 Li, R., Cui, L. L., Li, J. L., Zhao, A., Fu, H. B., Wu, Y., Zhang, L. W., Kong, L. D., and Chen, J.
595 M.: Spatial and temporal variation of particulate matter and gaseous pollutants in China during
596 2014-2016, *Atmos Environ*, 161, 235-246, 10.1016/j.atmosenv.2017.05.008, 2017b.
- 597 Liu, F., Zhang, Q., A., R. J. v. d., Zheng, B., Tong, D., Yan, L., Zheng, Y., and He, K.: Recent
598 reduction in NO_x emissions over China: Synthesis of satellite observations and emission
599 inventories, *Environ Res Lett*, 11, 114002, 2016.
- 600 Liu, Y., Yuan, B., Li, X., Shao, M., Lu, S., Li, Y., Chang, C. C., Wang, Z., Hu, W., Huang, X.,
601 He, L., Zeng, L., Hu, M., and Zhu, T.: Impact of pollution controls in Beijing on atmospheric
602 oxygenated volatile organic compounds (OVOCs) during the 2008 Olympic Games: observation
603 and modeling implications, *Atmos Chem Phys*, 15, 3045-3062, 2015.
- 604 Liu, Z., Wang, Y., Gu, D., Zhao, C., Huey, L. G., Stickel, R., Liao, J., Shao, M., Zhu, T., Zeng,
605 L., Amoroso, A., Costabile, F., Chang, C. C., and Liu, S. C.: Summertime photochemistry during
606 CAREBeijing-2007: RO_x budgets and O₃ formation, *Atmos Chem Phys*, 12, 7737-7752,
607 10.5194/acp-12-7737-2012, 2012.
- 608 Lu, X., Hong, J. Y., Zhang, L., Cooper, O. R., Schultz, M. G., Xu, X. B., Wang, T., Gao, M.,
609 Zhao, Y. H., and Zhang, Y. H.: Severe surface ozone pollution in China: A global perspective,
610 *Environ Sci Tech Lett*, 5, 487-494, 2018.
- 611 Mellor, G. L., and Yamada, T.: Development of a turbulence closure model for geophysical fluid
612 problems, *Rev Geophys*, 20, 851-875, 1982.
- 613 Morcrette, J. J., Barker, H. W., Cole, J. N. S., Iacono, M. J., and Pincus, R.: Impact of a new
614 radiation package, McRad, in the ECMWF Integrated Forecasting System, *Mon Weather Rev*,
615 136, 4773-4798, 10.1175/2008mwr2363.1, 2008.
- 616 Morrison, H., Thompson, G., and Tatarskii, V.: Impact of cloud microphysics on the
617 development of trailing stratiform precipitation in a simulated squall line: Comparison of one-
618 and two-moment schemes, *Mon Weather Rev*, 137, 991-1007, 10.1175/2008MWR2556.1, 2009.
- 619 Myneni, R., Knyazikhin, Y., and Park, T.: MCD15A2H MODIS/Terra+Aqua Leaf Area
620 Index/FPAR 8-day L4 Global 500m SIN Grid V006, in, NASA EOSDIS Land Processes DAAC,
621 <https://doi.org/10.5067/MODIS/MCD15A2H.006>, 2015.
- 622 Otero, N., Sillmann, J., Schnell, J. L., Rust, H. W., and Butler, T.: Synoptic and meteorological
623 drivers of extreme ozone concentrations over Europe, *Environ Res Lett*, 11, 024005, 2016.
- 624 Pu, X., Wang, T. J., Huang, X., Melas, D., Zanis, P., Papanastasiou, D. K., and Poupkou, A.:
625 Enhanced surface ozone during the heat wave of 2013 in Yangtze River Delta region, China, *Sci
626 Total Environ*, 603, 807-816, 2017.

- 627 Ren, Y., Qu, Z. L., Du, Y. Y., Xu, R. H., Ma, D. P., Yang, G. F., Shi, Y., Fan, X., Tani, A., Guo,
628 P. P., Ge, Y., and Chang, J.: Air quality and health effects of biogenic volatile organic
629 compounds emissions from urban green spaces and the mitigation strategies, *Environ Pollut*,
630 230, 849-861, 2017.
- 631 Saha, S., et al.: The NCEP Climate Forecast System version 2, *J Climate*, 27, 2185-2208,
632 10.1175/JCLI-D-12-00823.1, 2013.
- 633 Shao, M., Lu, S. H., Liu, Y., Xie, X., Chang, C. C., Huang, S., and Chen, Z. M.: Volatile organic
634 compounds measured in summer in Beijing and their role in ground-level ozone formation, *J*
635 *Geophys Res-Atmos*, 114, 2009.
- 636 Sillman, S.: The use of NO_y, H₂O₂, and HNO₃ as indicators for ozone-NO_x-hydrocarbon
637 sensitivity in urban locations, *J Geophys Res-Atmos*, 100, 14175-14188, 1995.
- 638 Sillman, S.: The relation between ozone, NO_x and hydrocarbons in urban and polluted rural
639 environments, *Atmos Environ*, 33, 1821-1845, 1999.
- 640 Soriano, J. B., et al.: Global, regional, and national deaths, prevalence, disability-adjusted life
641 years, and years lived with disability for chronic obstructive pulmonary disease and asthma,
642 1990-2015: a systematic analysis for the Global Burden of Disease Study 2015, *Lancet Resp*
643 *Med*, 5, 691-706, 10.1016/S2213-2600(17)30293-X, 2017.
- 644 Stavrakou, T., Muller, J. F., Bauwens, M., De Smedt, I., Van Roozendaal, M., Guenther, A.,
645 Wild, M., and Xia, X.: Isoprene emissions over Asia 1979-2012: Impact of climate and land-use
646 changes, *Atmos Chem Phys*, 14, 4587-4605, 10.5194/acp-14-4587-2014, 2014.
- 647 Sun, L., Xue, L., Wang, Y., Li, L., Lin, J., Ni, R., Yan, Y., Chen, L., Li, J., Zhang, Q., and Wang,
648 W.: Impacts of meteorology and emissions on summertime surface ozone increases over central
649 eastern China between 2003 and 2015, *Atmos Chem Phys*, 19, 1455-1469, 10.5194/acp-19-1455-
650 2019, 2019.
- 651 Sun, W. X., Hess, P., and Liu, C. J.: The impact of meteorological persistence on the distribution
652 and extremes of ozone, *Geophys Res Lett*, 44, 1545-1553, 10.1002/2016gl071731, 2017.
- 653 Tonnesen, G. S., and Dennis, R. L.: Analysis of radical propagation efficiency to assess ozone
654 sensitivity to hydrocarbons and NO_x 1. Local indicators of instantaneous odd oxygen production
655 sensitivity, *J Geophys Res-Atmos*, 105, 9213-9225, 2000.
- 656 Wang, J., Zhao, B., Wang, S., Yang, F., Jia, X., Morawska, L., Ding, A., Kulmala, M.,
657 Kerminen, V. M., and Kujansuu, J. J. S. o. t. T. E.: Particulate matter pollution over China and
658 the effects of control policies, 584-585, 426, 2017.

- 659 Wang, Q. G., Han, Z. W., Wang, T. J., and Zhang, R. J.: Impacts of biogenic emissions of VOC
660 and NO_x on tropospheric ozone during summertime in eastern China, *Sci Total Environ*, 395,
661 41-49, 10.1016/j.scitotenv.2008.01.059, 2008.
- 662 Wang, S. X., Zhao, B., Cai, S. Y., Klimont, Z., Nielsen, C. P., Morikawa, T., Woo, J. H., Kim,
663 Y., Fu, X., Xu, J. Y., Hao, J. M., and He, K. B.: Emission trends and mitigation options for air
664 pollutants in East Asia, *Atmos Chem Phys*, 14, 6571-6603, DOI 10.5194/acp-14-6571-2014,
665 2014.
- 666 Xing, J., Wang, S. X., Jang, C., Zhu, Y., and Hao, J. M.: Nonlinear response of ozone to
667 precursor emission changes in China: A modeling study using response surface methodology,
668 *Atmos Chem Phys*, 11, 5027-5044, 2011.
- 669 Yang, X., Xue, L. K., Wang, T., Wang, X. F., Gao, J., Lee, S. C., Blake, D. R., Chai, F. H., and
670 Wang, W. X.: Observations and explicit modeling of summertime carbonyl formation in Beijing:
671 Identification of key precursor species and their Impact on atmospheric oxidation chemistry, *J*
672 *Geophys Res-Atmos*, 123, 1426-1440, 2018.
- 673 Zhang, G., Gao, Y., Cai, W., Leung, L. R., Wang, S., Zhao, B., Wang, M., Shan, H., Yao, X.,
674 and Gao, H.: Seesaw haze pollution in North China modulated by the sub-seasonal variability of
675 atmospheric circulation, *Atmos Chem Phys*, 19, 565-576, 10.5194/acp-19-565-2019, 2019.
- 676 Zhang, J. X., Gao, Y., Luo, K., Leung, L. R., Zhang, Y., Wang, K., and Fan, J. R.: Impacts of
677 compound extreme weather events on ozone in the present and future, *Atmos Chem Phys*, 18,
678 9861-9877, 10.5194/acp-18-9861-2018, 2018.
- 679 Zhang, Q., Yuan, B., Shao, M., Wang, X., Lu, S., Lu, K., Wang, M., Chen, L., Chang, C. C., and
680 Liu, S. C.: Variations of ground-level O₃ and its precursors in Beijing in summertime between
681 2005 and 2011, *Atmos Chem Phys*, 14, 6089-6101, 10.5194/acp-14-6089-2014, 2014.
- 682 Zhang, Y. Z., and Wang, Y. H.: Climate-driven ground-level ozone extreme in the fall over the
683 Southeast United States, *Proc Natl Acad Sci USA*, 113, 10025-10030,
684 10.1073/pnas.1602563113, 2016.
- 685 Zhao, B., Wang, S. X., Liu, H., Xu, J. Y., Fu, K., Klimont, Z., Hao, J. M., He, K. B., Cofala, J.,
686 and Amann, M.: NO_x emissions in China: Historical trends and future perspectives, *Atmos*
687 *Chem Phys*, 13, 9869-9897, DOI 10.5194/acp-13-9869-2013, 2013.
- 688 Zhao, B., Wu, W. J., Wang, S. X., Xing, J., Chang, X., Liou, K. N., Jiang, J. H., Gu, Y., Jang, C.,
689 Fu, J. S., Zhu, Y., Wang, J. D., Lin, Y., and Hao, J. M.: A modeling study of the nonlinear
690 response of fine particles to air pollutant emissions in the Beijing-Tianjin-Hebei region, *Atmos*
691 *Chem Phys*, 17, 12031-12050, DOI 10.5194/acp-17-12031-2017, 2017.

- 692 Zhao, B., Zheng, H. T., Wang, S. X., Smith, K. R., Lu, X., Aunan, K., Gu, Y., Wang, Y., Ding,
693 D., Xing, J., Fu, X., Yang, X. D., Liou, K. N., and Hao, J. M.: Change in household fuels
694 dominates the decrease in PM_{2.5} exposure and premature mortality in China in 2005-2015, Proc
695 Natl Acad Sci USA, 115, 12401-12406, 2018.
- 696 Zhao, S. P., Yu, Y., Yin, D. Y., He, J. J., Liu, N., Qu, J. J., and Xiao, J. H.: Annual and diurnal
697 variations of gaseous and particulate pollutants in 31 provincial capital cities based on in situ air
698 quality monitoring data from China National Environmental Monitoring Center, Environ Int, 86,
699 92-106, 10.1016/j.envint.2015.11.003, 2016.
- 700 Zheng, B., et al.: Trends in China's anthropogenic emissions since 2010 as the consequence of
701 clean air actions, Atmos Chem Phys, 18, 14095-14111, 2018.
- 702 Zheng, G. J., Duan, F. K., Su, H., Ma, Y. L., Cheng, Y., Zheng, B., Zhang, Q., Huang, T.,
703 Kimoto, T., Chang, D., Poschl, U., Cheng, Y. F., and He, K. B.: Exploring the severe winter haze
704 in Beijing: the impact of synoptic weather, regional transport and heterogeneous reactions,
705 Atmos Chem Phys, 15, 2969-2983, 2015.
- 706